



# SRC 2021





# UNIVERSITY of HOUSTON

---

EARTH AND ATMOSPHERIC SCIENCES

34<sup>TH</sup> ANNUAL



**STUDENT RESEARCH CONFERENCE  
AND  
ALUMNI & INDUSTRY OPEN HOUSE**

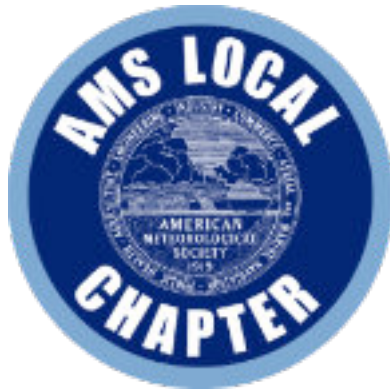
---

**APRIL 30, 2021**

---

# Table of **CONTENTS**

Schedule of Events .....	<b>1</b>
Oral Presentations .....	<b>2</b>
Morning.....	<b>2</b>
Session 1 .....	<b>2</b>
Session 2.....	<b>4</b>
Session 3.....	<b>6</b>
Afternoon.....	<b>8</b>
Session 1 .....	<b>8</b>
Session 2.....	<b>9</b>
Keynote Speaker .....	<b>10</b>
Abstracts .....	<b>12</b>
Student Committee .....	<b>28</b>
Judges .....	<b>30</b>
Acknowledgements.....	<b>31</b>



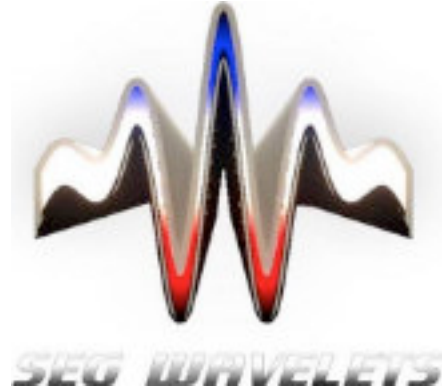
*American Meteorological Society*  
UHStudentAMS@gmail.com



*AAPG Wildcatters*  
AAPG.Wildcatters@gmail.com



*GeoSociety*  
GeoSocietyatUH@gmail.com



*SEG Wavelets*  
SEGWavelets@gmail.com



*AEG @ AIPG*  
AEGatUH@gmail.com



# Schedule @ **LOGISTICS**

*Zoom Meeting links and passcodes will be emailed to you upon RSVP.*

<b>MORNING SESSIONS</b>	9:00 am - 12:15 pm
<b>INTERMISSION</b>	10:30 - 10:45 am
<b>LUNCH BREAK</b>	12:15 - 1:00 pm
<b>AFTERNOON SESSIONS</b>	1:00 - 2:30 pm
<b>INTERMISSION</b>	2:30 - 3:30 PM
<b>KEYNOTE SPEAKER</b>	3:30 - 4:00 pm
<b>AWARDS CEREMONY</b>	4:00 - 5:00 pm
<b>HAPPY HOUR</b>	5:30 pm - 9:00 pm

*Our happy hour is optional for all faculty, students, alumni, and industry members to join:*

**McGONIGEL'S MUCKY DUCK**  
2425 NORFOLK STREET  
HOUSTON, TX 77098

## 2 • MORNING SESSION 1

---

### **9:00 AM**

*Rachel Clark*

Marine sedimentary records of Holocene changes along the margin of Thwaites Glacier, Amundsen Sea, West Antarctica

### **9:15 AM**

*Yuesu Jin*

Observation of transient fluid pressure amplification in a fluid-filled fracture

### **9:30 AM**

*Lucien Nana Yobo*

Strontium isotope response during OAE 2

### **9:45 AM**

*Weiyao Yan*

A new concordia age for the 'forearc' Bay of Islands Ophiolite Complex, Western Newfoundland utilizing spatially-resolved LA-ICP-MS U-Pb analyses of zircon

### **10:00 AM**

*Hualing Zhang*

Integration of basin analysis and gravity modeling for the Sergipe-Alagoas rifted-passive margin, northeastern Brazil

### **10:15 AM**

*Muhammad Nawaz Bugti*

Hydrocarbon generation and source rock maturity modeling along the Port Isabel Passive Margin Foldbelt, Northwestern Gulf of Mexico

**10:45 AM**

*Stephanie Suarez*

Pb and Rb-Sr isotope systematics of enriched components in Tissint

**11:00 AM**

*Md Nahidul Hasan*

Thermal Maturity Modeling of the Tithonian Source Rocks Along the Campeche Salt Basin, Southern Gulf of Mexico

**11:15 AM**

*Yi-Wei Chen*

Plate reconstruction of the proto-Caribbean since the mid-Cretaceous from unfolded-slab tectonics

**11:30 AM**

*Suoya Fan*

Megathrust Heterogeneity, Crustal Accretion, and Topographic Embayment in the Western Nepal Himalaya: Insights from the Inversion of Thermochronological Data

**11:45 AM**

*Mei Liu*

Crustal thickness variations of the Greater Gulf of Mexico region from integrated geological and geophysical analysis

**12:00 PM**

*Sean Romito*

Testing the transitional crust and its implications on the tectonomagmatic evolution of the Camamu-Almada margin along the northeastern rift segment of Brazil

**9:00 AM**

*Michael Daniel*

Structural Evolution of the Western Nepal Fault System: How does a splay fault evolve in a thrust wedge?

**9:15 AM**

*Michael Comas*

Sedimentary Record of Recent Retreat of Pine Island Glacier, Amundsen Sea, Antarctica

**9:30 AM**

*Rodrigo Alatorre*

Monterey Microplate: Fossil Slab or Lithospheric Drip below southern California?

**9:45 AM**

*Veronica Zermeno*

Detrital Zircon Geochronology and Sediment Provenance of Late Cretaceous Stratigraphy in the Western Interior Basin

**10:00 AM**

*Halina Haider*

Comparison of different hyperspectral remote sensing methods for Central Texas Outcrops

**10:15 AM**

*Steven Ramirez*

Quantifying subduction rates in the Pacific basin since the mid-Cretaceous (100Ma)



**10:45 AM**

*Aldair Machado*

Economic Analysis of Girassol Prospect, Angola

**11:00 AM**

*Kenneth Shipper*

Kinematic framework of shear stress variations along the San Andreas strike-slip fault zone

**11:15 AM**

*Nikola Bjelica*

Hiatus Mapping in Texas

**11:30 AM**

*Alvaro Iglesias*

Diagenetic Study of Jurassic Navajo Sandstone “Bleaching” Mechanisms

**11:45 AM**

*Mary Catherine Hambrick*

Smear Slide Analysis to Assess Variability of  $^{210}\text{Pb}$  Dates in Sediment Cores from Offshore Thwaites Glacier, Antarctica

**12:00 PM**

*Nabeel Muhammedy*

Using Multivariate Linear Regression to Estimate Permeability from Thin Section Image Analysis

**9:00 AM**

*Madeline Statkewicz*

Changes in Daily Precipitation in Houston, Texas

**9:15 AM**

*Wei Li*

Identification of Sea Breeze Recirculation and Its Effects on Ozone in Houston, TX, During DISCOVER-AQ 2013

**9:30 AM**

*Ellen Creedy*

The Global Radiant Energy Budgets of Titan and Mars

**9:45 AM**

*Arman Pouyaei*

Development and implementation of a physics-based convective mixing scheme in the CMAQ modeling framework

**10:00 AM**

*Claudia Bernier*

Cluster analysis of multi-dimensional ozone lidar measurements in coastal environments toward evaluating ozone simulations

**10:15 AM**

*Yannic Lops*

Application of a Partial Convolutional Neural Network for Estimating Geostationary Aerosol Optical Depth Data

**10:45 AM**

**Olabosipo Osibanjo**

Anatomy of the March 2016 Severe Ozone Smog Episode in Mexico City

**11:00 AM**

*Elizabeth Klovenski*

Understanding the Effect of Drought on Biogenic Isoprene and the Biosphere-Atmosphere-Chemistry Relationship with NASA GISS ModelE+MEGAN Simulations

**11:15 AM**

*Jia Jung*

Role of sea fog over the Yellow Sea on air quality with the direct effect of aerosols

**11:30 AM**

*Osman Tirmizi*

Hazard Potential in Southern Pakistan: A Study on the Subsidence and Neotectonics of Karachi and Surrounding Areas

**11:45 AM**

*Bavand Sadeghi*

Characterization of the volatile organic compounds in Houston petrochemical area: seasonal variability, source apportionment and regional transport

**12:00 PM**

*Kamil Qureshi*

Neotectonics study of the Main Frontal Thrust: An example from the Manzai Ranges in the Northwestern Himalayas, Pakistan

## 8 • AFTERNOON SESSION 1

---

### **1:00 PM**

*Andrew Stearns*

Quantifying Hurricane Harvey Sediment Transport in The Houston-Galveston Region

### **1:15 PM**

*Lila Bishop*

Progressive, along-strike deformation and stratigraphic response of the Central American Forearc basin

### **1:30 PM**

*Bryan Moore*

Along-strike structure of the Barbados accretionary prism: The structural effects of subducting bathymetric highs on wedge taper angle, prism growth, and hydrocarbon potential

### **1:45 PM**

*Tanzina Akther*

Volatile Organic Compounds (VOCs) Mixing Ratios in Mexico City During a Severe Ozone Episode

### **2:00 PM**

*Irfan Karim*

Case study analyses of PM<sub>2.5</sub> in Lahore, Pakistan, using in-situ air quality and remote sensing data

### **2:15 PM**

*Mahmoudreza Momeni*

Developing a Four-Dimensional Variational Framework to Refine Estimates of Ammonia Emissions



**1:00 PM**

*Sharif Morshed*

Stress and frequency dependent properties of poroelastic anisotropic

**1:15 PM**

*Benjamin Miller*

Tectonic evolution of the Cenozoic Lesser Antilles volcanic arc

**1:30 PM**

*Sharmila Appini*

Verification of Predicted Shear wave splitting due to Strong Seismic Anisotropy in subduction slabs

**1:45 PM**

*Sara Rojas*

Evaluating Hurricane Harvey's Erosional Impact on the Sand Dunes of San Luis Pass

**2:00 PM**

*Moloud Rahimzadeh Bajgiran*

Applying cluster analysis to seismic tomography models: "Uncovering the presence of compositional anomalies"

**2:15 PM**

*Sriharsha Thoram*

Updated bathymetry map of Tamu Massif, northwest Pacific: Implications on the ocean plateau formation at triple junction and post-shield volcanic activity

# *Dr. Ny Riavo Voarintsoa* **KEYNOTE SPEAKER**



**DR. NY RIAVO VOARINTSOA** (aka Voary), originally from Madagascar, obtained a PhD degree in Geology in 2017 at the Department of Geology at the University of Georgia (UGA). After receiving her PhD, she went to the Institute of Earth Sciences of the Hebrew University in Jerusalem in Israel (HUJI) for a post doc position (2017-2019), then was awarded the Marie Curie Fellowship by the European Horizon to continue research at the Department of Earth and Environmental Sciences of the Katholieke Uniersiteit Leuven (or KU Leuven) (2019-2021). Much of her research has been focused on paleoclimate and paleoenvironmental reconstruction using various proxies archived in stalagmites in tropical regions. Specifically, such research was aimed at understanding the dynamic of the Intertropical Convergence Zone (ITCZ), which is the main driver of monsoon rainfall in the region. Currently, Voary is a Research Assistant Professor at the Department of Earth and Atmospheric Sciences of the University of Houston in Texas, where she plans to develop a clumped isotope and triple oxygen isotope proxy to refine paleoclimate reconstruction in tropical regions.



# THE POWER OF GEOSCIENCES IN PREDICTING PAST CLIMATE

Climate and environmental changes are among important challenges facing our society today. To better prepare for the future, we need to understand how climate has changed in the past, with a range beyond instrumental records, because this is our reference knowledge to refine future climate simulations. To do this, we need geological materials. Overall, our understanding of past climate changes depends on (1) developing and calibrating reliable proxies from one or more geological archives to reconstruct the changes, (2) selecting a climate sensitive region where such archives are available, and (3) linking together paleoclimate records from several locations worldwide to test and evaluate climate models. My keynote presentation will highlight the importance of stalagmites, secondary cave deposits, from Madagascar to understand how our climate has changed in the past. It will report on the most recent proxy calibration performed in Anjohibe cave, our study site in northwestern Madagascar, and the application of stable oxygen isotope proxy to understand monsoon rainfall, that is linked to the latitudinal migration of the Inter-tropical Convergence Zone. I will conclude my talk by introducing some challenges in the reconstruction and by discussing newer opportunities to address them in future work.

*The keynote speech will take place from 3:30 - 4:00 PM.*



## UNDERGRADUATE GEOLOGY

### Rodrigo Alatorre

#### *Monterey Microplate: Fossil Slab or Lithospheric Drip below southern California?*

The birth of the San Andreas transform plate boundary resulted in the Farallon plate fragmenting into the Juan de Fuca and Cocos plates and smaller microplates such as the Monterey, Guadalupe, and Magdalena microplates along the coast of California and Baja California, Mexico. Although subduction of these microplates has ceased, proposed fossil slabs still connected to these extinct trenches have sparked debate. In this study, we use recent mantle tomographic imaging to map and structurally unfold lost Cocos and Monterey microplate lithosphere back to Earth's surface. The Isabella anomaly is a controversial high velocity structure beneath the Southern Great Valley of California which has been proposed to represent either delaminated material from the Sierra Nevada batholith or a fossil slab connected to the Monterey microplate. To test these interpretations, we use recent surface wave tomography to map and structurally unfold the Isabella anomaly. Our results show the length of the anomaly is ~350 km, similar to the lengths of the Monterey microplate predicted from high-resolution seafloor isochrons. These results support the interpretation of a fossil slab which broke from the main Farallon plate at 28.2 Ma to create the Monterey microplate. Furthermore, we extend our restoration of ancient Farallon lithosphere by unfolding the Cocos slab present in the upper mantle below Mexico. Our results account for ~55 Ma of Cocos subduction, suggesting a change in subduction regime of the Farallon plate during early Cenozoic time.

### Mary Catherine Hambrick

#### *Smear Slide Analysis to Assess Variability of $^{210}\text{Pb}$ Dates in Sediment Cores from Offshore Thwaites Glacier, Antarctica*

Thwaites Glacier or the "Doomsday Glacier" is important because of its potential to contribute to rising sea levels. However, due to its remote location, little is known about its past glacial dynamics and variability. The goal of my research is to document recent glacial-marine changes over the past 100 years to better understand what factors control this glacier's stability. I will be working with marine sediment samples collected near the Thwaites Glacier floating ice shelf as the sediment records past glacial-marine changes. Using high-resolution observations of the sediment grain properties with smear-slide analysis, grain-size measurements, and radioactive isotope dating techniques, I hope to explore the variability and correlations in the glacial-marine sediments. Samples from two cores with prior dating analysis will be studied. The sediment samples will be coming from cores taken both at a seafloor high in 500 m water depth and deep trough at 1200 m depth. The  $^{210}\text{Pb}$  age data from the shallow site is not conclusive, so I will contribute high resolution analysis of the sediment to understand when the glacier's floating ice shelf lost contact with the seafloor. As for the deeper core site, I will use these same techniques to understand when this area was covered by the ice shelf and when that ice shelf retreated away from the site. The primary question going into this research is: Can I relate sediment deposition to the ratios of quartz, lithic fragments, and diatoms? The second question is: Will I detect a variability in my observations of different minerals with respect to the core and is it mutually exclusive to glacial retreat? I hypothesize that the mineralogy ratios will reflect the environments of deposition and the changes in mineralogy will indicate when the ice shelf retreated. The aim of the research is to observe the relationship between  $^{210}\text{Pb}$  dating and the variability of its mineralogical makeup and grain size in the marine sediments to determine the timing of ice retreat.

### Aldair Machado

#### *Economic Analysis of Girassol Prospect, Angola*

It is important to understand the risks and uncertainties involved in the development of exploration prospects, and how these impacts the outlook for profitability. Our case study is Girassol prospect in the Deepwater Congo Basin of Angola. The goal of this presentation is to characterize the economic outcomes of Girassol prospect in terms of recoverable hydrocarbons, discounted cash flow and economic metrics such as Internal Rate of Return (IRR) and Net Present Value (NPV). For a reasonable evaluation of the risks and uncertainties of this prospect, geologic risk elements and volumetric assessments are integrated into a forecast of costs, production/revenue, schedule, and oil price. The geologic and cost data for this project are based on published information. A thorough analysis of these risks and uncertainties is critical to obtain a clear perspective of the risked economics and the commerciality of the prospect. In terms of risking results, the geologic risk of Girassol was estimated at 40%, and an economic chance of success of 30%. Source Rock was the primary technical risk element which then required great condition for additional elements such reservoir, migration path and a seal. The assessed recoverable oil volumes were 925 million barrels (MMBO) for the economic mean with a p90 to p10 range of 560 to 1458 MMBO, based on a Monte Carlo simulation. In addition, three possible scenarios, based on tertiles were developed to represent low (599 MMBO), mid (833 MMBO), and high side (1342 MMBO) scenarios. The estimated productive areas associated with this analysis were 20km<sup>2</sup>, 53km<sup>2</sup>, and 82km<sup>2</sup> respectively. The economic mean success case yields an IRR of 20% and an NPV@10 of about 2.5 billion dollars. Risked economics (accounting for economic dry holes) yields an IRR of 13% and a positive NPV. Even the lowside (599 MMBO) case is economic, with a success case IRR = 18%. Incorporation of geological understanding into economic evaluations is fundamental to good decision making, especially in exploration. This includes a consideration of both risk and volumetric uncertainty.



**Steven Ramirez***Quantifying subduction rates in the Pacific basin since the mid-Cretaceous (100Ma)*

The reconstruction of subducted lithospheric plates is important to understand the behavior of current tectonic activity and its effect over long periods. The percentage of uncertainty increases as we go farther back in time, preventing accurate reconstructions of the subducted lithosphere. However, to date, no one has systematically quantified the amounts of subduction over time, and across individual subduction margins. This limitation has caused controversy over how to reconstruct the missing lithosphere accurately. This study aims to quantify the rate of subduction of the Pacific basin from the mid-Cretaceous (100 Ma) to the present. GPlates is a software program that enables interactive visualizations and manipulation of plate tectonics. For this study, the GPlates program was used to track the movements of the present-day Pacific basin back through time. Measurements were taken every 5 Ma of the uncertainty area formed between known subduction zones to track the relative area of the lithosphere that had been subducted. Our results show that an average of 1.36% of the Pacific basin subducted every 5 Ma since the mid-Cretaceous period. The rate of subduction among each region varies, since mid-Cretaceous the East Asian margin has an average subduction rate of 451,510.22 km<sup>2</sup>/Ma, with the Australian margin having a rate of 266,511.87 km<sup>2</sup>/Ma. On the opposite side of the Pacific basin at the northwestern North American margin, the average subduction rate since the mid-Cretaceous has been 145,810.93 km<sup>2</sup>/Ma, and the Central/South American margin average subduction rate is 456,400.04 km<sup>2</sup>/Ma. Data collected from this study will be applied to future studies in identifying and un-subducting lithosphere within the mantle.

**Veronica Zermeno***Detrital Zircon Geochronology and Sediment Provenance of Late Cretaceous Stratigraphy in the Western Interior Basin*

Late Cretaceous stratigraphic units in Wyoming and Montana record the transition from Sevier to Laramide orogenesis. Due to the absence of fossilized material in terrestrial or near shore deposits, constraining the timing of deposition and linking those deposits to their basinal equivalent has been difficult. Therefore, the goal of this study is to constrain depositional ages of terrestrial stratigraphy using U-Pb dating of detrital zircons. Geochronologic data will be gathered from published papers, maximum depositional ages (MDAs) will be calculated, and sediment provenance will be modeled using non-negative matrix factorization (NMF). These ages will be compared to biostratigraphic data in the basin. The results and interpretations will bring insight to sediment provenance in the Western Interior Basin and constrain time of deposition and temporal and spatial changes over time during partitioning of the Western Interior Basin during change of Sevier to Laramide orogenesis. Youngest single grain and youngest grain cluster at  $2\sigma$  uncertainty are the chosen methods to estimate MDAs for the terrestrial deposits. NMF modeling will be used to generate low-rank approximations of source distributions and identify key age populations present in the basin samples. Synthetic PDPs will be generated to represent possible sources to the basin.

**MASTERS ATMOSPHERIC SCIENCE****Tanzina Akther***Volatile Organic Compounds (VOCs) Mixing Ratios in Mexico City During a Severe Ozone Episode*

The Planetary Boundary Layer (PBL) acts as an important meteorological factor influencing pollutant's mixing ratio through dispersion and turbulent mixing processes. Here, we will present the diurnal variation of the PBL height and the impacts of the PBL height on Volatile Organic Compounds (VOCs) which in turn acts as a precursor of ozone formation in Mexico City from 6 to 18 March 2016. Two days (10 and 14 March 2016) have been chosen to represent quite different atmospheric scenarios: (1) strong winds and atmospheric mixing (10 March) and (2) weak winds and limited convection (14 March). On 10 March 2016, well mixed conditions due to elevated daytime PBL height and strong advection were observed. This led to overall reduced mixing ratios of CO (~0.2 ppm) and O<sub>3</sub> (~50 ppb) as well as for VOCs compared to preceding days. On 14 March 2016 weak wind speeds ( $\leq 5$  m/s) and rather limited convective processes were observed, which caused the accumulation of VOCs, NO<sub>x</sub> and CO, in particular under shallow nocturnal stable boundary layer conditions. This process was likely enhanced due nighttime drainage flows from the surrounding mountains into the basin of Mexico City. In addition, wind shear and air mass recirculation occurred within the basin. The combination of these chemical and meteorological processes led to high mixing ratios of O<sub>3</sub> (200 ppb) at daytime. At the same time, under solar radiation during daytime, lower mixing ratios of all the VOCs were observed on 14 March with lower PBL height compared to the preceding days. This suggests a relation of high O<sub>3</sub> mixing ratios with low VOCs mixing ratio as VOCs are reacting efficiently to produce ozone on that day. The benzene:toluene (b/t) ratio can be used as an indicator of traffic emission, as both aromatic compounds come from automobile exhaust. The b/t ratio was below 0.5 during the rush hour which is in agreement with other studies and indicates emission from motor vehicles. Ethylbenzene and the m/p-xylene isomers are emitted at typical ratios from the same sources. These aromatics only react with OH, however at different reaction rates. At daytime, due to photochemical reactions in the presence of strong solar radiation, this ratio increases as m,p-xylene reacts faster with OH than ethylbenzene. Both, on 10 and 14 March, there is a peak value in the e/m,p xylene ratio coinciding with the peak solar radiation around noontime. Moreover, there is even a further reduction of this ratio during daytime on 14 March indicating enhanced ozone formation on that day as m,p-xylene is one of the top VOCs producing ozone efficiently.

**Irfan Karim***Case study analyses of PM<sub>2.5</sub> in Lahore, Pakistan, using in-situ air quality and remote sensing data*

This study investigates observations of Particulate Matter (PM<sub>2.5</sub>) for Lahore, Pakistan, for selected case studies in the year 2020 with a combination of in-situ air quality data, aerosol optical depth (AOD) retrievals from satellite-based Moderate Resolution Imaging Spectroradiometer (MODIS), and AOD observations from the ground-based Aerosol Robotic Network (AERONET). This study is complemented by hybrid single-particle Lagrangian integrated trajectory (HYSPLIT) trajectories and National Center for Environmental Prediction (NCEP) reanalysis data set. Results indicated that the variations in the day-night PM<sub>2.5</sub> concentration was affected by the diurnal variations of both the emission intensity and the atmospheric physical and chemical processes. One such episode in Lahore is marked from 19th till 23rd March 2020, when peak PM<sub>2.5</sub> hourly concentration of about 500 $\mu\text{g}/\text{m}^3$  around 7 am correlated with elevated MODIS AOD and AERONET AOD. The Pakistan government announced a COVID-19 lockdown from March 23rd to May 31st, 2020. From May 27th to 30th PM<sub>2.5</sub> average hourly concentration at the surface level was below 60 $\mu\text{g}/\text{m}^3$ , while in contrast MODIS data observed have enhanced AOD values. After these episodes, pre-monsoon season started, and overall conditions got better. In-situ surface PM<sub>2.5</sub> and AOD data showed better relation for post monsoon (SON) than pre monsoon (MAM) conditions. The elevated AERONET and MODIS AOD values during the pre-monsoon period are likely due to high dust loading from the deserts of Cholistan and Thar (Pakistan) as supported by HYSPLIT and NCEP data while higher values during the post monsoon periods are attributed to anthropogenic/local activities. The intra-annual analysis shows the aerosol trend AERONET AOD remained higher with two peaks approximately 0.7 and 0.8 in the month of July.

**Mahmoudreza Momeni***Developing a Four-Dimensional Variational Framework to Refine Estimates of Ammonia Emissions*

Ammonia (NH<sub>3</sub>) plays a significant role in forming fine inorganic particulate matter (PM<sub>2.5</sub>) in the atmosphere, which is associated with premature mortality. Uncertainty in ammonia emissions is propagated into secondary PM<sub>2.5</sub> concentrations simulated by the model, which are used to estimate health effects. We are preparing a python-based four-dimensional variational framework to calculate revised estimates of NH<sub>3</sub> emissions with a combination of observations from the satellite-based instrument and chemical transport model with its adjoint. We first tested the validity of the adjoint-based sensitivities of concentrations with respect to emissions by comparing them to sensitivities calculated with the forward model using the finite difference method. Once confirmed, inorganic PM<sub>2.5</sub> and ammonia were simulated over East Asia using the chemical transport model. A cost function is defined to calculate the discrepancy between the satellite data and the model output using the gradient of it with respect to ammonia emissions. Then, the influences of emissions on the cost function are determined by using the adjoint of the model (inverse modeling). These spatially specific sensitivities are evaluated in different regions over East Asia. Finally, the model adjoint is integrated into the Python-based four-dimensional variational framework for future refinement of ammonia emissions over East Asia.

**MASTERS GEOPHYSICS****Sharmilla Appini***Verification of Predicted Shear wave splitting due to Strong Seismic Anisotropy in subduction slabs*

Decades ago, it was observed that many deep subduction earthquakes (depth > 60 km) show large non-double couple component (ndcc) in the results of moment tensor source analysis. These findings are used as a proof to argue that deep earthquakes rupture differently from shallow earthquakes. Recently, it was shown that there is a strong evidence of high seismic anisotropy in the vicinity of deep earthquakes (subducting slabs) which can cause the observed apparent ndcc. This discovery has motivated me to further investigate the existence of such anisotropy by studying the shear wave splitting (SWS) patterns of transmitted S waves through anisotropic slabs. Hence, I will make SWS predictions based on the inverted slab anisotropy from the moment tensors and compare the predicted outcomes with SWS observations. The initial hypothesis for this research is that the strong anisotropy in the dipping slabs can cause the observed different shear wave splitting patterns which critically depend on the back-azimuths of earthquakes as well as the slab anisotropy. It is in sharp contrast with many previous SWS studies which did not consider where the earthquake source is in the interpretation. I will evaluate this hypothesis in the Japan subduction zone with the following approach. Firstly, intra-slab anisotropy strength will be obtained using deep earthquake moment tensors. Then, SWS predictions will be made for both local and teleseismic waves using both 3D-anisotropic elastic finite difference modeling and a propagator matrix method. Finally, these predictions will be compared to the observed splitting measurements (polarization and delay time). For the Student Research Conference, I will be presenting the preliminary SWS results of teleseismic S waves through the Japan slab as a function of back-azimuth using SplitLab. These measurements will be further used to test the proposed hypothesis and find an intra-slab anisotropic model that can simultaneously explain both the earthquake radiation patterns and the observed SWS. The broader impact of this project will be to understand the slab anisotropy structure and the geological environment in which deep earthquakes occur.

### **Benjamin Miller**

#### *Tectonic evolution of the Cenozoic Lesser Antilles volcanic arc*

The largely submarine, Cretaceous to recent Lesser Antilles subduction system consists of the Aves Ridge remnant arc, the Grenada back-arc basin, the Lesser Antilles volcanic arc (LAVA), the Tobago forearc basin, and the Barbados accretionary prism. Several previous tectonic models have been proposed for the Late Cretaceous evolution of the Lesser Antilles subduction system along its 850-km-long trend. We tested three different tectonic models using three, 840-920-km-long, dip gravity transects and one 700-km-long, strike transect. Each gravity transect is constrained using previous seismic reflection and refraction data along with 500 radiometric age dates. Dredged samples of plutonic rocks from the Aves Ridge are dated as Campanian to Paleocene (78-57 Ma) and represent the earliest known volcanic arc magmatism of the Lesser Antilles volcanic arc. Rifting of the Grenada back-arc basin and Tobago forearc basin occurred during the early to middle Eocene with the formation of forearc, oceanic crust during the middle Eocene. Onlap of Oligocene clastic sediments against more steeply dipping Oligocene clastic sediments record the intrusion and emergence of the LAVA. The intrusion of the nascent LAVA entrained middle Eocene oceanic crust now exposed as fragments in the Grenadine Islands. Gravity data reveals that the southern LAVA with age dates of the latest Oligocene-early Miocene (24-20 Ma) bifurcates into two northern branches beginning at the island of Martinique and separating along the Miocene to recent Kallinago basin. The western, active branch (inner arc) shows a range of dates from Pliocene to recent (4-0 Ma), while the extinct, outer arc capped by limestone shows dates ranging from late Eocene to early Miocene (35-20 Ma). The tectonic model that best fits the gravity profiles and dates include 1) eastward shift about 190 km of the volcanic arc from the late Cretaceous Aves Ridge to its present-day location of the LAVA during the Oligocene; this eastward shift was likely a response to slab rollback; 2) westward shift from the inactive Limestone Caribbees to the active inner arc (13-5 Ma); this westward shift was likely a response to subduction of elevated areas of oceanic fracture zones.

### **Moloud Rahimzadeh Bajgiran**

#### *Applying cluster analysis to seismic tomography models: "Uncovering the presence of compositional anomalies"*

In recent years, several types of Machine Learning (ML) methods have been employed by Earth scientists to extract patterns and structures from multi-dimensional feature spaces. In this regard, images of the mantle obtained by different seismic tomography (ST) models are diverse datasets with varying structures due to their different theoretical approximations and input data. In this work, we apply an unsupervised ML method, K-means clustering, on ST models to explore their similarities and differences to improve our physical understanding of the Earth's interior. The K-means clustering method requires ST models to be standardized in a three-dimensional domain. For this purpose, we implement a weighted average technique to resample ST models to radial structural zones with uniform horizontal grid resolutions. However, the homogenized ST models still have  $10^3$ - $10^4$  parameters, which need to be distilled into a small number of summary features. Feature selection is thus a key part of this study: features should be independent from unphysical effects of inversion choices (e.g., the damping factor) and should instead capture the essence of the geological structure. Preliminary results obtained using the center of mass as the attribute to represent the longest wavelength part of the mantle structure show that P-wave and S-wave models do not cluster separately. Therefore, compositional anomalies do not play an essential role at these spatial scales. We plan to expand our analysis by including more summary attributes from both the spatial as well as the frequency domain.

### **Sara Rojas**

#### *Evaluating Hurricane Harvey's Erosional Impact on the Sand Dunes of San Luis Pass*

Coastal sand dune systems are an ever changing and crucial component for the survival of a coastlines ecosystem, providing vital protection from coastal erosion during typical wind and wave processes. For major events, such as hurricanes and tropical storms, these naturally forming barriers absorb the initial impact of high winds and storm surges, preventing or delaying the flow of waters inland. San Luis Pass, a strait between the east side of Follett's Island and the west side of Galveston Island, connects West Bay to the Gulf of Mexico. In Brazoria county, The Follett's Island is a known receding area containing artificial sand dunes. Whereas the west side of Galveston Island is comprised of naturally forming sand dunes and is an area of known accretion. This provides a unique situation; a location in which the perseverance of artificial and natural sand dunes, under relatively similar conditions, can be compared. This case study utilizes LiDAR to evaluate the erosional impact of Hurricane Harvey on the sand dunes of San Luis Pass. This study focuses on a limited area of the islands with the goal of developing a methodology for analyzing the sediment movement and elevation changes of this area, later to be expanded further along each island. The west end of Galveston Island exhibits a general overall decrease in elevation and a significant retreat of coastline. The remaining dry beach zone shows flattening of unvegetated windblown undulations along the coastline. Larger back dunes with vegetation shows less change in elevation, whereas smaller clusters of dunes with sparse amounts of vegetation show greater elevation reduction. Immediately after Harvey, sand can be seen transported further inland into previously visually vegetated areas. In comparison, the limited area examined for the east end of Follett's Island contains fewer dunes, but an overall decrease in elevation and significant retreat of coastline is also visible. The southern side of the San Luis Toll Bridge contains a few larger dunes topped with smaller dunes; areas with denser vegetation, or near the vegetation line, also show smaller elevation changes.

## MASTERS GEOLOGY

### Lila Bishop

#### *Progressive, along-strike deformation and stratigraphic response of the Central American Forearc basin*

The forearc basin along the Middle America trench extends along the western edge of the Caribbean plate and overlies the subducting Cocos plate. The basin consists of two segments: the undeformed, 800-km-long submarine and undeformed forearc basin from northern Guatemala to the Nicoya Peninsula of northwestern Costa Rica and the inverted and subaerial (0-1000m ASL), 300-km-long segment that includes the Tempisque and Terraba belts of Costa Rica. I have made four regional structural transects in the 630-km-long structural transition zone between the two segments to show that the Eocene through Miocene lithologies, facies, and depositional environments are the same in both the undeformed and inverted segments of the forearc basin. Inversion of the southeastern segment is related to Oligocene to recent subduction of the Cocos Ridge and its precursor, oceanic plateaus that were generated by the Galapagos hotspot. Our subsurface dataset that is centered on the structure transition area and includes 77 2D, time-migrated, newly acquired and reprocessed industry and academic seismic lines, and the age-dated, Corvina-2, offshore well log. Using these data, we document an Oligocene-recent folding event marked by a regional, angular unconformity and are associated with a 200-km-long, a 30-km-wide, trench-parallel belt of fault propagation folds. Syn-folding, sandy deposits document abrupt shallowing across the unconformity from depths of 3000 m to shallower depths of ~250m as measured from clinoforms. From seismic facies interpretation of the sigmoid and oblique clinoforms, I document the Miocene – recent shelf margin evolution. Miocene infill of the basin is slightly oblique to the W-SW. In the Pliocene, subduction of the Cocos Ridge and Panama Triple Junction (PTJ) changes the basin configuration; the basin progrades and infills to the NW.

### Nikola Bjelica

#### *Hiatus Mapping in Texas*

It has been proposed that Texas experienced uplift and tilt during the latter part of the Cenozoic based on onlapping strata and truncated sequences. The precise timing, spatial extent, and amplitude of these vertical motions, as well as their dynamic causes, remain poorly constrained. We propose to analyze regional-scale unconformities from geologic maps and regional cross-sections of Texas to compile hiatus maps at spatial scales of many hundreds of kilometers and at temporal scales of geologic epochs. This will be complemented by the analysis of subsurface geometries and by a quantitative assessment of the role of post-rift thermal subsidence and lithospheric flexure induced by sediment loading. Our analysis will put additional constraints on the timing and amplitude of tilting, refining our knowledge of the tectonic history of Texas. Additionally, we will be able to assess whether changes in dynamic support from the convecting mantle are required to explain these past vertical motions of the Texas lithosphere.

### Michael Comas

#### *Sedimentary Record of Recent Retreat of Pine Island Glacier, Amundsen Sea, Antarctica*

Models of future glacial behavior suggest that the West Antarctic Ice Sheet (WAIS) may be poised for collapse within the next 200 years. While there is currently no certainty to how quickly this retreat may occur, investigation of previous glacial dynamics may hold the key to how the WAIS may respond to future climate variability. Observations in the Amundsen Sea Embayment in West Antarctica have inspired recent investigation into the drivers of this phenomenon and the rate at which it can be expected to continue. The glaciers of primary concern within the Amundsen Sea Embayment are Thwaites Glacier and Pine Island Glacier. Both of these glaciers have been experiencing ice shelf thinning and grounding-line retreat since at least the beginning of satellite data acquisition. This study seeks to understand how Pine Island Glacier has receded during the Holocene by employing several different investigative methods on sediment cores collected proximal to Pine Island's ice shelf in February of 2020 alongside marine geophysical data. The location of these cores next to a recently calved portion of the shelf will allow for the study of newly exposed sediments. Initial core descriptions suggest that the retreat of Pine Island Glacier's grounding line may have been preserved where very poorly sorted diamicts are overlain by finer-grained, well-sorted sediments. Detailed analysis of grain size and shape will be conducted to reconstruct past glacial environments within Pine Island Bay along with radio-isotopic dating methods. Measurements of  $^{210}\text{Pb}$  within the sediments and  $^{14}\text{C}$  from foraminiferal tests allow for the construction of age models to establish times and rates of sediment deposition in the area. Initial  $^{210}\text{Pb}$ -dating indicates that the upper portions of the selected cores likely contain a record of recent retreat. Comparison of sedimentological analysis to detailed multibeam bathymetric data of the embayment provide a context of glacial dynamics in the region. Investigation into these sedimentological characteristics will help to uncover how Pine Island Glacier has changed in the recent past, and how it may react to climate in the future.



### **Michael Daniel**

#### *Structural Evolution of the Western Nepal Fault System: How does a splay fault evolve in a thrust wedge?*

The newly discovered and seismically active Western Nepal Fault System (WNFS) is hypothesized to be a subaerial thrust wedge system, transferring dextral strain from the Karakoram Fault in the obliquely convergent NW Himalayan 'backarc' to the central Himalayan 'forearc' where convergence is primarily margin normal. Based on observations made from both numerical modelling as well as field observations, we hypothesize the WNFS branches down from the Gurla Mandhata extensional system cutting through western Nepal via strike-slip faults and extensional step-overs. On the basis geologic and remote sensing observations, the WNFS is observed to consist of five to six different segments of strike-slip faults and extensional step-overs. However, the geometry, kinematics, and fault linkage of the WNFS is currently unknown except for at a few sites. Furthermore, evidence for thrusting along splay faults parallel to the observed strike-slip faults suggest that the WNFS may instead be related to thrusting, including deformation above lateral and frontal ramps on the megathrust. These observations open the door for many questions which we seek to answer in this study: (1) How do fault segments that make-up the WNFS link to become a through-going splay fault? (2) How does a splay fault evolve in a thrust wedge? (3) Is the splay fault linked to the megathrust, and, if so, how does this system link to the megathrust (4) Do the strike-slip segments show any evidence of thrusting prior to strike-slip motion? We propose a multi-disciplinary approach in which microstructural analysis, field work, and remote sensing will be implemented to address these questions. I propose three models to explain the surficial linkage of the two youngest segments of the WNFS in the south near Tansen: (1) The Propagating model, (2) The Pure-shear Model, and (3) The Simple-shear model. These models will serve as a general guideline for how and where we will conduct our traverses in the field. These results along with field mapping of the tectonostratigraphic sequences will be integrated along with previously published geologic maps to create a 3D geologic model of the WNFS.

### **Halina Haider**

#### *Comparison of different hyperspectral remote sensing methods for Central Texas Outcrops*

Recently, remote sensing to characterize and classify outcrops has grown exponentially to become a vital tool in studying the surface. Remote sensing technology provides a new outlook on the methods of acquiring and analyzing spatial, spectral and temporal resolutions. In this study, ground-based hyperspectral data, for four geological outcrops in central Texas, are processed and analyzed to compare and determine which method of classification yields the best and most accurate results. Data from each outcrop are analyzed to answer specific questions unique to these central Texas localities, including the possible weathering effects on spectra in Lion Mountain as well as petrogenesis of Pack Saddle Schist in Llano. Methods including spectral angle mapper (SAM), support vector machine (SVM) and artificial neural network (ANC) are focused on for classifying the data. Ground truth is established by spectra collected on samples using an ASD spectroradiometer in the laboratory as well as a geochemical analysis conducted using a portable X-Ray Fluorescence machine (pXRF). Classification results of the four outcrops show that SAM produces realistic and overall accurate results in comparison to SVM and ANC. Spectra collected from samples obtained from the Lion Mountain outcrop shows effects of weathering.

### **Alvaro Iglesias**

#### *Diagenetic Study of Jurassic Navajo Sandstone "Bleaching" Mechanisms*

The Navajo Sandstone is a Jurassic-aged, primarily eolian deposit, considered one of the largest such deposits in Earth's geologic record. This sandstone is unique in that it shows a variety of colors, including red, yellow, brown, and white. These coloration patterns are related to primary diagenetic hematite cement distribution around sand grains, where darker colors represent layers relatively enriched in the hematite cement and lighter colors represent layers relatively depleted in the cement. The process that determines the cement distribution throughout the formation is under debate, primarily on the basis of secondary diagenetic hematite reduction, dissolution and migration mechanisms. These mechanisms are typically referred to as "bleaching", as it resembles the bleaching of dark clothing to more pale colors. Previous literature on the re-precipitation of dissolved hematite cement into iron-oxide nodules at various outcrops of the Navajo Sandstone can help in understanding these secondary diagenetic mechanisms. Using remote sensing imagery, GIS data and geochemical data, these "bleaching" mechanisms can be determined at local outcrop resolution. By determining the bleaching mechanisms of multiple outcrop localities, it may be possible to infer this bleaching phenomenon at a regional scale.

**Bryan Moore***Along-strike structure of the Barbados accretionary prism: The structural effects of subducting bathymetric highs on wedge taper angle, prism growth, and hydrocarbon potential*

Critical taper of an accretionary prism is a function of various parameters that include wedge physical properties, pore fluid pressure, slab dip, strength of the fault, incoming sediment thickness and deformational effects of subducting bathymetric highs. This study focusses on lateral changes of the critical taper, friction along the subduction detachment, and strength of the wedge material within the 50-300-km-wide and 10-20-km-thick, Barbados accretionary prism and the prism's response to the oblique subduction of two, elongate, oceanic fracture zone-related basement highs (Tiburón Rise and Barracuda Ridge). To describe the prism geometry and to understand these complex relationships, I use: 1) GEBCO 2020 bathymetric data to map the effects of the basement highs on the deformation front; 2) USGS Slab2 Benioff zone surface to provide the deeper, subduction zone geometry; and 3) a compilation of multi-channel seismic lines to constrain the shallower structure of the prism and the structure of the subducting oceanic crust and its overlying sedimentary cover. These combined datasets allow for the measurement of the prism surface slope ( $\alpha$ ) vs. the dip of the top of the subducting plate ( $\beta$ ) angles that are then used to calculate lateral variations in the internal wedge strength and in the frictional strength of the basal detachment. The resulting calculations reveal the effects of bathymetric highs on wedge taper angles that include: 1) closer spaced and imbricated thrust faults and associated folds along the areas of the deformation front that are in contact with the two subducting highs; 2) damming of the voluminous, clastic sediment supply from the Orinoco River that ponds along the southward slopes of the two fracture zone ridges and produce abrupt widening in the prism's zone of frontal accretion - that in turn increases the wedge taper angles; 3) areas of bathymetric highs show an increased taper angle from  $5^{\circ}$ - $10^{\circ}$  while regions that lack thick trench sediments exhibit prism taper angles from  $4^{\circ}$ - $8^{\circ}$ . For the effects of the oblique ridge subduction on the distribution of hydrocarbons within the prism, I use a 2D grid of 16,367 line-kms of multi-channel seismic data provided by MultiClient Geophysical to compile locations of all direct hydrocarbon indicators (DHIs) from the three main structural provinces of the prism: 1) the zone of frontal accretion along which Atlantic sediments are actively accreting today; 2) the zone of initial stabilization in the center of the prism where imbricated thrust slices have been rotated to vertical; and 3) the zone of piggyback basins and westward backthrusting along the western edge of the prism.

**Andrew Stearns***Quantifying Hurricane Harvey Sediment Transport in The Houston-Galveston Region*

Hurricane Harvey made landfall as a Category 4 hurricane in Port Aransas, Texas on August 26, 2017 and produced the largest precipitation event in recorded US history over Houston and Southeastern Texas. Harvey stalled southwest of the Houston area from August 28-30 after weakening to a tropical storm, resulting in over 20,347 km<sup>2</sup> of Texas receiving more than 0.75 m (30 in) of precipitation. The ensuing runoff caused mobilization of large sediment volumes within fluvial-estuarine systems in the Houston-Galveston region. I carried out an integrated quantitative analysis to determine the total net sediment transported in the Houston-Galveston area during Hurricane Harvey using pre- and post-Harvey digital elevation models (DEMs), satellite and ground-based images, and sediment dredging reports along major waterways. The 6.21 km<sup>3</sup> of precipitation in 12 fluvial-estuarine and 2 controlled reservoir drainages in the Houston-Galveston area mobilized a minimum of 27,227,448 m<sup>3</sup> of sediment, equivalent to 6-51 and 30-118 years of annual discharge to Galveston Bay, compared to the modern and the Holocene, respectively. Harvey transported the equivalent 15.5 Astrodomes, 1/3 of the annual sediment load delivered to the Gulf of Mexico by the Mississippi River sediment, and 16% of the size of Galveston island above sea level. Nearly 26% of the transported sediment was deposited in the flood controlled Addicks and Barker reservoirs located 50 km West of downtown Houston, decreasing their overall holding capacity by 1.2% and 1.6%, respectively. Out of 154,170 homes flooded in Harris County, 10,000 were within the two reservoirs. These homes face increasing flood risk from decreasing reservoir capacities due to sediment infilling and increasing impervious areas. In the stream drainages, sediment was transported from higher elevations West-Northwest of Houston to lower elevations towards Galveston Bay. Sediment deposited downstream within stream banks decreases bankfull volume capacities and increases future susceptibility to flooding. In addition, the magnitude of net sediment transport decreases as the degree of channel modification increases. Natural channels tend to disrupt the surrounding urban area by retaining sediment in its floodplains through overbank deposition while artificially straightened channels bypass sediment into downstream navigable channels.

## PH.D. ATMOSPHERIC SCIENCE

### Claudia Bernier

*Cluster analysis of multi-dimensional ozone lidar measurements in coastal environments toward evaluating ozone simulations*

Large surface ozone variations are frequently observed in coastal regions which makes the modeling of air quality in these regions challenging. The ability to properly model coastal regions relies heavily on the proper detailed observations. There have been three air quality studies (over Chesapeake Bay and the Long Island Sound) that focused on thorough measurements in these complex coastal regions; OWLETS 1 & 2 and LISTOS. Over the course of the campaigns, there were surface ozone observations taken from LIDAR (Light Detection And Ranging) instruments for a total of 91 days at a high temporal rate. We developed a clustering method that characterizes vertical profile ozone measurements by its temporal and vertical ozone behavior specific to these coastal regions. We identified 6 vertical profile clusters and used the developed clusters to validate two chemical transport models: GEOS-Chem and GEOS-CF.

### Ellen Creecy

*The Global Radiant Energy Budgets of Titan and Mars*

Radiant energies of planets and moons are of wide interest in the fields of geoscience, astronomy, and planetary sciences. Examining radiant energy budgets gives insight into atmospheric thermal structure, atmospheric circulation, and weather and climate patterns. The radiant energy budget for terrestrial bodies is determined by the emitted thermal energy and absorbed solar energy. Here, we present our current work measuring the energy budgets of Titan and Mars. Titan is the only satellite in our solar system with a thick atmosphere, made of mostly nitrogen, as well as an active methane cycle that produces large permanent liquid bodies on the surface. Mars has many unique features that affect energy transport mechanisms, such as polar ice caps, large-scale dust storms, large orbital eccentricity (0.0935), and large obliquity (25.19°). Both of these terrestrial bodies have complex characteristics that create a very interesting energy budget picture. For Titan, we use long-term multi-instrument Cassini observations covering three Titan seasons (2004-2017) to examine the seasonal variations of the global energy budget. For Mars, we are using observations from the Thermal Emission Spectrometer (TES) onboard the Mars Global Surveyor (MGS) and the Mars Climate Sounder (MCS) onboard the Mars Reconnaissance Orbiter (MRO) to investigate the radiant energy budget from 1997 to 2020. We found that Titan's global-average emitted power decreased by  $6.8 \pm 0.4\%$  during the Cassini period, while the total absorbed solar power decreased  $18.69 \pm 0.11\%$ . Therefore, the global-average emitted energy is not balanced by the absorbed solar energy, with an average global energy imbalance of  $2.73 \pm 0.46\%$ . In addition to our work with Titan, we are currently conducting the first long-term observational studies of Mars' energy budget using MGS/TES (1997-2006) and MRO/MCS (2006-). Given the many factors that influence energy transport and thermal structure on Mars, we believe that Mars has a significantly dynamic energy budget. Studies covering Mars' radiant energy budget are relatively few, with focus near the polar region. Our preliminary results using TES and MCS observations are promising, and we believe our research will give insight into the red planet's energy dynamics.

### Jia Jung

*Role of sea fog over the Yellow Sea on air quality with the direct effect of aerosols*

In this study, we investigate the impact of sea fog over the Yellow Sea on air quality with the direct effect of aerosols for the entire year of 2016. Using the WRF-CMAQ two-way coupled model, we perform four model simulations with the up-to-date emission inventory over East Asia and dynamic chemical boundary conditions provided by hemispheric model simulations. During the spring of 2016, prevailing west-southwesterly winds and anticyclones caused the formation of a temperature inversion over the Yellow Sea, providing favorable conditions for the formation of fog. The inclusion of the direct effect of aerosols enhanced its strength. On foggy days, we find dominant changes of aerosols at an altitude of 150-200 m over the Yellow Sea resulted by the production through aqueous chemistry ( $\sim 12.36\%$  and  $\sim 3.08\%$  increases in sulfate and ammonium) and loss via the wet deposition process ( $\sim 2.94\%$  decrease in nitrate); we also find stronger wet deposition of all species occurring in PBL. Stagnant conditions associated with reduced air temperature caused by the direct effect of aerosols enhanced aerosol chemistry, especially in coastal regions, and it exceeded the loss of nitrate. The transport of air pollutants affected by sea fog extended to a much broader region. Our findings show that the Yellow Sea acts as not only a path of long-range transport but also as a sink and source of air pollutants. Further study should investigate changes in the impact of sea fog on air quality in conjunction with changes in the concentrations of aerosols and the climate.

**Elizabeth Klovenski***Understanding the Effect of Drought on Biogenic Isoprene and the Biosphere-Atmosphere-Chemistry Relationship with NASA GISS ModelE+MEGAN Simulations*

Drought is a hydroclimatic extreme that causes perturbations to the terrestrial biosphere. As a stressor for vegetation, drought can induce changes to vegetative emissions known as BVOCs (Biogenic Volatile Organic Compounds). Biogenic isoprene represents about half of total BVOC emissions and is a precursor to ozone ( $O_3$ ) and secondary organic aerosol (SOA), both of which are climate forcing species. In order to simulate isoprene during drought and the feedbacks associated with these complex BVOC-chemistry-climate interactions, we implemented the MEGAN<sub>3</sub> (Model of Emissions of Gases and Aerosols from Nature) isoprene drought stress parameterization in NASA GISS (Goddard Institute of Space Studies) ModelE, a leading Earth System Model. New diagnostics are programmed into ModelE to allow for the evaluation of the algorithm's performance and comparisons to limited isoprene flux measurements and satellite derived HCHO (formaldehyde) column. Offline and online drought stress simulations will be used to demonstrate the effect of the parameterization.

**Wei Li***Identification of Sea Breeze Recirculation and Its Effects on Ozone in Houston, TX, During DISCOVER-AQ 2013*

In coastal environments, sea breeze recirculation has been found to be an important mesoscale meteorological phenomenon that causes high ozone episodes, yet the identification of this small-scale circulation pattern remains difficult. In this study, a new method was developed to automatically identify sea breeze recirculation in Houston, TX by applying K-Means clustering algorithm to surface winds measurements at near-coast sites during the DISCOVER-AQ (Deriving Information on Surface Conditions from Column and Vertically Resolved Observations Relevant to Air Quality) field campaign period from August to October 2013. The key to the clustering algorithm is seven features derived from site-based surface winds on each day, including zonal (U) and meridional (V) winds in the morning and afternoon, 24-h transport direction ( $\Theta$ ) and the recirculation factor, which is the ratio of net transport distance (L) to wind run distance (S). For comparison, the same clustering was applied to San Antonio, TX, a non-coastal city yet within the synoptic-scale distance from Houston. Four clusters were obtained for each region, including three synoptic patterns common to both regions and one mesoscale pattern that differs by region, classified as Stagnation and Sea Breeze Cluster for San Antonio and Houston, respectively. The clustering outputs were verified by wind profiler data in Houston. By linking the wind clusters with surface and aircraft ozone measurements, we revealed a clear connection between circulation patterns and daily ozone variability showing that maximum daily average 8-hr (MDA8) ozone levels and spatial distributions differed by cluster type (e.g., the highest ozone found in the Stagnation/Sea Breeze Cluster and the lowest ozone in the Southerly Cluster). This automatable method of sea breeze identification we developed can be potentially applied to other coastal cities because it has low data requirement and no ad hoc location-specific adjustments.

**Yannic Lops***Application of a Partial Convolutional Neural Network for Estimating Geostationary Aerosol Optical Depth Data*

Satellite-derived aerosol optical depth is negatively impacted by cloud cover and surface reflectivity. As these issues lead to biases, they need to be discarded, which significantly increases the amount of missing data within an image. This paper presents a unique application of the partial convolutional neural network (partial CNN) for imputing missing data from the Geostationary Ocean Color Imager (GOCI) by training the partial CNN model with the Community Multiscale Air Quality model simulated AOD. The partial CNN model outperforms the Kriging Gaussian process regression method by up to 9.6% for imputing GOCI images and up to 17% based on AERONET measurements. Once trained, the model requires significantly less processing time and fewer resources than the Kriging method. Furthermore, the model allows the use of higher temporal resolutions of remote sensing data in further research, for example, on data assimilation techniques and human health impact analysis.

**Olabosipo Osibanjo***Anatomy of the March 2016 Severe Ozone Smog Episode in Mexico City*

The diurnal evolution of the planetary boundary layer (PBL) is crucial to air quality studies as it impacts the exchange and distribution of pollutants close to the surface. This paper reports continuous detection of the daytime convective boundary layer height, the stable boundary layer height, and the residual layer height as estimated from the vertical profiles of virtual potential temperature, and moisture retrieved from a microwave radiometer (MWR) in Mexico City for the period 6-18 March 2016. This period included a severe smog episode. We analyzed the anatomy of this episode utilizing continuous air quality measurements recently deployed at elevated locations surrounding the basin of Mexico City, which were used to determine the impact of the background or residual pollutants during the severe smog episode in combination with back trajectory analysis and radar wind profiles data to track transport processes within the Mexico City basin. The first few days prior to the smog episode were impacted by the passage of a deep upper tropospheric trough and strong advection. Shortly before the smog episode, daytime maximum PBL height still reached ~2.5 km above ground level but then dropped to ~1.2-1.7 km above ground level for the most severe pollution days. During the first days with strong advection, the pollutant concentrations were flushed out from the basin and/or could not accumulate (maximum hourly ozone and carbon monoxide mixing ratios of ~50 ppbv and ~0.5 ppmv, respectively). At the departure of the storm, the winds became weaker, and a strong near surface temperature inversion was observed at nighttime increasing the nighttime mixing ratio of carbon monoxide to ~2.5 ppmv and daytime ozone mixing ratio to ~200 ppbv, which resulted in one of the most severe smog episodes in Mexico City over the last decade. Our results point to strong photochemical processes confined to the PBL within the Mexico City basin, whose maximum daytime convective boundary layer heights hardly surpassed the surrounding average mountain top heights.



**Arman Pouyaei***Development and implementation of a physics-based convective mixing scheme in the CMAQ modeling framework*

To improve the representation of convective mixing of atmospheric pollutants in the presence of clouds, we developed a convection module based on Kain and Fritsch (KF) method and implemented it in the CMAQ (Community Multiscale Air Quality) model. The KF-convection method is a mass-flux based model that accounts for updraft flux, downdraft flux, entrainment, detrainment, and the subsidence effect. We apply the KF-convection model to an idealized case and to a reference setup prepared for East Asia during the KORUS-AQ campaign period to investigate its impact on carbon monoxide (CO) concentration at various atmospheric altitudes. A comparison of the results of the standard CMAQ with the KF-convection model for convection days reveals two types of impacts from KF-convection; a direct impact caused by vertical movement of CO concentrations by updraft or downdraft and an indirect impact caused by transport of lifted CO concentrations to another region. May-12 saw a high indirect impact originated from the Shanghai region at higher altitudes and a high direct impact of updraft fluxes at 1 km altitude. However, May-26 revealed an immense updraft increasing higher altitude concentrations (up to 40 ppbv) and diverse indirect impacts over the region of the study ( $\pm 50$  ppbv). The overall comparison shows a strong connection between differences in the amount of concentration caused by the direct impact at each altitude with the presence of an updraft at that altitude. The developed model can be employed in large domains (i.e., East Asia, Europe, North America, and Northern Hemisphere) with sub-grid scale cloud modeling to include the convection impacts.

**Bavand Sadeghi***Characterization of the volatile organic compounds in Houston petrochemical area: seasonal variability, source apportionment and regional transport*

In an integrated characterization study of the Automated Gas Chromatograph (AutoGC) monitoring stations for the Houston metropolitan area, the hourly measurements of volatile organic compounds (VOCs) were analyzed for summertime and wintertime 2018. The average concentration of total VOC compounds was 28.68 ppbc for summertime and 33.92 ppbc for wintertime. Alkane compounds had the largest contributions, which accounted for 61% and 82% of VOCs in summertime and wintertime respectively. Positive Matrix Factorization (PMF) identified seven VOC factors in the summertime and six factors in the wintertime among which alkane species formed three factors according to their rate of reactions in both seasons: (1) the emissions of long-lived tracers from oil and natural gas (ONG long-lived species), (2) fuel evaporation, and (3) emissions of short-lived tracers from oil and natural gas (ONG short-lived species). Two other mutual factors were (4) emissions of aromatic compounds and (5) alkene tracers of ethylene and propylene. Summertime factor (6) was associated with acetylene and wintertime factor (6) was affected by the emissions of vehicle exhausts. An additional factor of (7) biogenic emissions was influenced by the presence of isoprene in the summertime that could be from the intensive effects of high temperature and solar radiation. While the industrial complexes and refineries were the main contributors to the measured VOC, summertime higher ratios of ethylene to acetylene indicated the stronger impacts of photochemical reactivity with hydroxyl radical. The CWT showed the contributions of Baytown and Galveston refineries as potential sources of ONG long-lived factor during the summertime and wintertime.

**Madeline Statkewicz***Changes in Daily Precipitation in Houston, Texas*

There has been an alarming increase in the frequency of major flooding events along the Gulf Coast over the last three decades, primarily due to events of unprecedented, or extreme rainfall. Using data from 63 rain gauges maintained by the Harris County Flood Warning System (FWS), this study examines the changes in daily precipitation events in the highly urbanized city of Houston, Texas, USA. The potential shift in annual precipitation patterns over a period of three decades (1989-2018) was examined by investigating the numbers of dry and wet days (e.g., R20, R50, R100) as well as daily precipitation totals over the study period. Wet days were then further scrutinized based on daily rainfall amounts to determine if extreme events are beginning to dominate annual rainfall amounts. Trends were analyzed for statistical significance using the Mann-Kendall and Sen's slope methods and for spatial trends using GIS applications. The results indicate a statistically significant increase in extreme rainfall at the expense of light, moderate, and heavy rainfall over time. The only negative relationship found is in dry days. The most statistically significant increases are seen for the 99th percentile and for R100, with increases of 0.729 [units of 99th percentile] and 0.02 days per year. There has been strong growth and development in the Houston area in recent decades, and land cover change has been significant. In fact, urbanization has continued to increase while total vegetative and wetland coverage have decreased. The findings of this study provide guidance for city and state planners and engineers.

**PH.D. GEOPHYSICS****Sharif Morshed***Stress and frequency dependent properties of poroelastic anisotropic*

The poroelastic response of fluid saturated porous rock due to stress variations is of interest as it has practical applications in reservoir depletion, fluid injection, time-lapse monitoring, and carbon dioxide sequestration. The effective stress in a poroelastic medium relates to applied pressure and pore pressure, with the Biot parameter ( $\alpha$ ) as a scaling factor of the pore pressure. This work offers an independent derivation of the tensor characteristics of  $\alpha$  through elastic moduli, a microscopic effective medium derivation, and frequency-dependent behavior of  $\alpha$  for an anisotropic medium. We derived simplified equations for isotropic rock subjected to confining pressure and pore pressure, isotropic rock under uniaxial stress considering the nonlinear part of elastic constants, and an equation of  $\alpha$  for the frequency-dependent case. In the effective medium derivation, we assumed that the rock contains both isolated pores and connected pores saturated with liquid. We use the GSA method to Barnett shale core samples to link ultrasonic velocities with mineral composition and porosity data. We corroborate our theoretical formulations by applying those equations to experimental data for different scenarios such as changes in confining pressure, pore pressure, and uniaxial stress. We calculated the Biot tensor for sandstone and shale. We found excellent agreement between theoretical prediction and experimental data. It is known that  $\alpha$  varies significantly for changes in porosity and rock microstructure in isotropic rock. We also see as much as a 21% difference between horizontal and vertical components of  $\alpha$  for transversely isotropic (TI) rock for changes in uniaxial stress. We then estimated the frequency-dependent Biot tensor for TI models using numerical calculations. We noticed significant differences between vertical ( $\alpha_{33}$ ) and horizontal ( $\alpha_{11}$ ) components of  $\alpha$ , especially at the surface seismic frequency band. However, uniaxial stress and horizontally aligned microstructure influence the elastic moduli and Biot tensor contrarily. In general, anisotropy due to uniaxial stress shows lower  $\alpha_{33}$  and higher  $\alpha_{11}$ . The anisotropy due to microstructure shows the opposite.

**Sriharsha Thoram***Updated bathymetry map of Tamu Massif, northwest Pacific: Implications on the ocean plateau formation at triple junction and post-shield volcanic activity*

Shatsky Rise is a large oceanic plateau in northwest Pacific located ~1600 km east of Japan. It consists of three large edifices: Tamu, Ori and Shirshov massifs. Tamu Massif is the largest and the oldest edifice and is at the southwest end of the plateau. Oceanic plateaus like Shatsky Rise are massive crustal basaltic emplacements widely considered to have formed from massive eruptions from the surfacing of a deep mantle plume. Magnetic lineations surrounding the plateau imply that Tamu Massif formed at the Pacific-Farallon-Izanagi triple junction. Recently magnetic lineations have also been found inside Tamu Massif suggesting a complex ridge-hotspot interaction involved in its formation. Studying geomorphology can reveal important clues in the formation of Tamu Massif but has been historically very limited due to enormous size and remote location. We conducted an extensive multibeam survey over Tamu Massif onboard R/V Falkor (cruise FK151005) during which we collected ~6 x 10<sup>6</sup> new soundings. In addition, we acquired about ~17 x 10<sup>6</sup> new multibeam soundings from other agencies (NCEI and JAMSTEC databases) and combined them with satellite predicted bathymetry data to generate a new high-resolution bathymetry map of Tamu Massif. The new map shows Tamu Massif to be segmented, with the main edifice flanked by four lower rises separated by subdued troughs. These troughs are probably abandoned spreading centers caused by ridge jumps during the reorganization of the triple junction that accompanied Tamu Massif formation. The map also reveals presence smaller volcanic ridges, volcanic cones and clusters overprinting the massif, probably a result of secondary volcanism. In addition, we identified aerially extensive mass wasting features, such as sediment slumps and creep folds, disturbing the sediment cover of the massif. High-resolution bathymetry reveals new details about both the large-scale formation of the volcanic plateau but also about previously hidden details of post-volcanic evolution and sedimentation.

**PH.D. GEOLOGY****Muhammad Nawaz Bugti***Hydrocarbon generation and source rock maturity modeling along the Port Isabel Passive Margin Foldbelt, Northwestern Gulf of Mexico*

The northeast-southwest trending Port Isabel passive margin foldbelt spans over an area of 17,000 square kilometers in the deepwater Gulf of Mexico. Only a few wells are drilled in the area that resulted in one uncommercial hydrocarbon discovery in the well PI#525. The abnormally thick Oligocene section prevented drilling activity from penetrating the known source rocks. The petroleum systems in the area are poorly understood, and the current study tries to identify potential rocks. The authors initially constructed 1D petroleum systems models for all drilled wells. Later, 2D models were generated using TrinityTM along a key regional seismic line considering Upper Jurassic, Upper Cretaceous, and the Wilcox shales as source rocks in the area. The selection of source rocks is speculative considering undrilled stratigraphy below Oligocene. Seismic data constrained the stratigraphic depth and thickness. The model's assumptions are a) homogeneous heat source from the basement, b) No differentiation made between radiogenic basement heat and heat from mantle convection, c) assuming heat was transferred by conduction and by water expelled vertically during compaction, and d) bottom-hole temperatures suggest higher heat flow values than the surrounding areas. We also made unrestrained models and compensated by the assumption of extreme cases of high and low scenarios to account for the uncertainty due to the scarcity of drilled stratigraphy. Series of maps are created illustrating source rock maturity and transformation ratios for Tithonian, Upper Cretaceous, and Paleogene source rocks. Hydrocarbon charge volumes were also estimated for each drilled well, treated as a prospect, with their respective fetch areas and the uncertainty captured through Monte Carlo simulation. At the same time, the 2D seismic profile reveals hydrocarbon generation history through various stages of deformation.

### Yi-Wei Chen

#### *Plate reconstruction of the proto-Caribbean since the mid-Cretaceous from unfolded-slab tectonics*

Located between North and South America, the Caribbean is a large igneous province (CLIPs) bounded by active plate margins, possibly formed at the Galapagos hot spot in the Late Cretaceous. From the Galapagos to its current location, the eastward motion of the CLIPs would have consumed at least ~3000 km long and ~2000 km wide oceanic lithosphere that was originally occupied between the Americas, the so-called proto-Caribbean oceanic lithosphere. However, only one third (~1100 km) of the proposed size was found previously in a global seismic tomography at the present Lesser Antilles subduction zone. Here, we used a recently published S-wave full-waveform tomography, US-32 to map out the mantle structure underneath the Caribbean. Besides the previously found Lesser Antilles slab, we also found a new sub-horizontal fast anomaly at 450 km depth underneath the Caribbean to the west of the Lesser Antilles slabs. We also reconstructed the pre-subducted plate configurations with spreading ridges and fracture zones based on the patterns of the velocity perturbation transferred onto our mapped slabs. We found this new sub-horizontal anomaly has an area comparable with the missing proto-Caribbean lithosphere. The proposed spreading ridge configurations are consistent with the predictions from synthetic isochrones and are also consistent with the overriding plate geology. OIB and NMORB type magmatism were found at the central Hispaniola, where the spreading ridge intercepted the overriding plate, while the rest of the Greater Antilles arc experienced continuous arc magmatism from the late Cretaceous to the Eocene. The size of the slab and the pre-subducted plate configurations support that this newly found slab-like anomaly is the missing proto-Caribbean lithosphere.

### Rachel Clark

#### *Marine sedimentary records of Holocene changes along the margin of Thwaites Glacier, Amundsen Sea, West Antarctica*

Antarctica's contribution to global sea-level rise is predominantly due to ice-mass loss of the marine-based West Antarctic Ice Sheet in the Amundsen Sea drainage basin, often referred to as its "weak underbelly." Current thinning and retreat of ice streams in this sector, especially of Thwaites Glacier (TG), which may already be undergoing collapse, is largely attributed to warm water impinging onto the shelf and melting of buttressing ice shelves from below. Predictive ice-sheet and sea-level models require a strong understanding of controls on glacier mass balance, including ocean forcing and subglacial bed conditions. These factors can be understood through the study of past records of glacial change. During two research cruises, the former bed of TG was investigated by undertaking geophysical surveys and collecting marine sediment cores. The cores are used to investigate how TG has changed throughout the Holocene. Detailed core descriptions, grain size data, magnetic susceptibility, and CT scans allow for defining various lithological facies, which are utilized for reconstructing different glaciomarine environments close to the modern ice margin. Many cores across the region solely consist of laminated mud with sparse gravel and sand grains, suggesting meltwater plume deposition under open marine conditions or ice-shelf cover. Cores collected from bathymetric highs, close to the modern iceberg calving margin, transition from gravely sandy mud at the core base into thick laminated mud extending to the surface. This trend is interpreted to reflect the recent unpinning of the TG ice shelf from these seafloor highs. Two radioisotope systems,  $^{210}\text{Pb}$  and  $^{14}\text{C}$ , are used to constrain the rate of sediment accumulation and timing of glacial change in the region. Short-lived isotope geochronology, using  $\text{Pb-210}$ , shows that sediment accumulation rates vary spatially across the rough inner continental shelf from 0.5 to 3.6 cm per decade. Rates vary within individual cores, implying different depositional processes are active through time. Although the glacier including its front is changing rapidly today, radiocarbon age models imply that the TG margin has remained near its present-day position for much of the Holocene.

### Suoya Fan

#### *Megathrust Heterogeneity, Crustal Accretion, and Topographic Embayment in the Western Nepal Himalaya: Insights from the Inversion of Thermochronological Data*

The Himalayan range is remarkably uniform in its structure and topography along strike. However, between  $81^{\circ}30'$  E and  $83^{\circ}$  E these properties depart from its "perfect" arcuate shape and define a large-scale embayment. We hypothesize that deep tectonics along the megathrust at mid-lower crustal depths plays a lead role in growth of the embayment as well the southern margin of the Tibetan plateau. To investigate the merits of this hypothesis we conducted thermokinematic modeling of thermochronologic data from a topographic and structural embayment in the western Nepal Himalaya. We present a new suite of zircon (U-Th)/He thermochronologic analyses that are integrated with previously published data to investigate the three-dimensional geometry and kinematics of the megathrust at mid-lower crustal depths. Models that can best produce observation-fitting cooling ages suggest that the megathrust in the western Nepal Himalaya is characterized by two ramps connected by a long flat that extends further north compared to adjacent segments. The new data and modeling result suggest that the high slope zone along the embayment lies above the foreland limb of an antiformal crustal accretion zone on the megathrust with lateral and oblique ramps at mid-lower crustal depths. The lateral and oblique ramps may have initiated by ca. 10 Ma. This process may have controlled along-strike variation in plateau growth and therefore development of the topographic embayment. We compare the three-dimensional geometry of the megathrust that we obtained with geological and morphologic features and propose a conceptual evolution model for the landscape and drainage systems across the central-western Himalaya. Our work highlights the important role of crustal accretion or duplexes at different depths in orogenic wedge growth and that the mid-lower crustal accretion determines the plateau edge.

### **Md Nahidul Hasan**

#### *Thermal Maturity Modeling of the Tithonian Source Rocks Along the Campeche Salt Basin, Southern Gulf of Mexico*

Extending over 700 km along the southern Gulf of Mexico (GOM), the Campeche salt basin remains one of the least explored and drilled areas of the GOM basin. The objectives of this study include: 1) to image and structurally restore the morphology of the top of Paleozoic crystalline basement; 2) to understand the role of Paleozoic orogenic basement architecture and Triassic-Jurassic rift structures on total sediment thickness; and 3) to determine the relationship of crustal thickness and its related heat flow variations for the thermal maturity of source rocks within the basin. In this study, a grid of 23,600 line-km of 2D seismic reflection profiles with published wells and potential fields data have been used. The potential fields data was processed to provide an improved image of the subsalt top basement surface at a depth of 6-15 km. The top basement morphology is a northward-dipping, subsalt surface in the depth range of 6-15 km. The top basement map reveals the 40-55-km-wide Campeche segment of the 670-km long GOM marginal rift, formed by necking of continental crust prior to the formation of late Jurassic oceanic crust. The elongate and fault-bounded basement depression of the marginal rift combined with the presence of "step-up fault" on its seaward edge onto more elevated Jurassic oceanic crust is imaged in high resolution using the tilt derivative of the Bouguer anomaly. Mapping of 2D seismic lines reveals approximately 2-7 km of total sediment thickness along the slope of the Yucatan carbonate platform, which thickens up to 15 km along the marginal rift axis. A crustal thickness model of the Campeche salt basin from gravity inversion indicates a thickness of ~10-20 km in the thinned continental crust beneath the marginal rift and ~20-35 km in the less extended continental crust underlying the Yucatan carbonate platform. In this study, I present basin models in various sub-basins of the study area that takes into account the heat flow variations related to crustal thickness variations in the marginal rift and its adjacent, rifted, continental crust. A compilation of direct hydrocarbon indicators from these sub-basins supports our proposed areas of maturity.

### **Yuesu Jin**

#### *Observation of transient fluid pressure amplification in a fluid-filled fracture*

We proposed a new hypothesis called pressure surge (PS) effect as an explanation about a long-lasting puzzle that the earthquake can be triggered by small stress perturbations (~KPa). The PS effect states that the pressure inside the fluid-filled fracture can be amplified up to 2~3 orders of magnitude larger than the pressure of the incident wave. The amplification makes it possible that the small amplitude seismic waves can trigger earthquakes in regions where the fluid reservoirs are abundant. Our current laboratory work aims at verifying the pressure surge effect by low-frequency underwater acoustic experiment. We designed and built two novel instruments including an adjustable low-frequency source and high-sensitivity pressure sensors with only 0.2mm thickness. With these two critical instruments, we can generate single frequency incident wave and measure the fluid pressure inside the fracture directly. In current stage, we have already observed that the wave can be amplified by 25 times larger. The potential applications of pressure surge effect include geothermal monitoring, subsurface fracture imaging and earthquake hazard mitigation.

### **Mei Liu**

#### *Crustal thickness variations of the Greater Gulf of Mexico region from integrated geological and geophysical analysis*

Triassic-Jurassic continental rifting and seafloor spreading between North America and Yucatan block has produced the present-day basin morphology of the Gulf of Mexico (GOM). This study investigates the crustal structure and the distribution of crustal types, the history of rifting and seafloor-spreading, and the role of pre-existing crustal fabric on this evolution. I use ~90,000 km of 2D seismic grids, gravity data, full-tensor gravity gradiometry, 45 wells, and 178 previous seismic refraction stations to constrain a regional 3D gravity and tectonic model. The Moho inversion was constrained using the seismic refraction data and density inversions of the crustal and upper mantle layers. The inversion results indicate that the late Jurassic oceanic crust underlying the deep GOM ranges from 4-10 km in thickness and a new continent-ocean boundary was identified using the crustal thickness map. Stretch factors around the margin vary from 0-7 assuming that crustal thicknesses > 35 km remained undeformed during continental rifting. From this map, I have divided the Greater GOM area into four different crustal provinces based on these inversion results: 1) undeformed continental crust northwest of the Marathon Ouachita orogenic belt with a stretch factor of 1 and crust thicker than 35 km; 2) less deformed continental crust beneath the onshore areas that border the GOM with a stretch factor between 2-3 with a thickness between 20-35 km; 3) thinned continental crust in more distal settings with a thickness between 10-20 km and stretch factor between 3-5; and 4) late Jurassic, oceanic crust in the deep, central GOM that is less than 10 km thick. I use the palinspastic restoration of the extended continental crust within the conjugate margins to derive the restored continent-ocean boundary. The result suggests that the continental rifting occurred initially in an NW-SE direction prior to the late Jurassic, counterclockwise rotation phase of GOM opening. I overlay giant oil field locations and source rock distributions onto the crustal thickness map. This comparison reveals "sweet spots" – or crustal lows in the extended, continental - around the Greater GOM region.

**Lucien Nana Yobo***Strontium isotope response during OAE 2*

Ocean anoxic events are characterized by increased organic richness of marine sediment on a global scale with accompanying positive excursions in sedimentary organic and inorganic carbon isotope values. Increased supplies of nutrients to the oceans are required to sustain elevated levels of marine productivity necessary to account for high carbon export fluxes during ocean anoxic events. Submarine eruptions of one or more large igneous provinces are the proposed trigger for OAE 2, and the CO<sub>2</sub> induced global warming and increased rainfall acidification are both factors that can increase continental weathering rates and therefore nutrient inputs to the oceans. On the other hand, seawater interactions with hot basalts at LIP eruptions sites can deliver ferrous iron and other metals and reduced gases to seawater that can stimulate increased productivity in surface waters and increased oxygen demand in deep waters. The relative importance of continental and submarine weathering drivers of expanding ocean anoxia during OAE 2 are difficult to disentangle. In this talk, we present a new high-resolution record of seawater <sup>87</sup>Sr/<sup>86</sup>Sr in a pelagic carbonate succession from the Eagle Ford Formation in Texas. With the help of a box model of the ocean Sr cycle, and knowledge of the contrasting <sup>87</sup>Sr/<sup>86</sup>Sr signatures of continental weathering and submarine weathering inputs of Sr to the oceans, the relative magnitudes of the continental weathering and submarine weathering fluxes of Sr to the oceans during OAE 2 is determined. Finally, the new <sup>87</sup>Sr/<sup>86</sup>Sr data offers a significant refinement to the temporal pattern of changing <sup>87</sup>Sr/<sup>86</sup>Sr in the global ocean over OAE2.

**Kamil Qureshi***Neotectonics study of the Main Frontal Thrust: An example from the Manzai Ranges in the Northwestern Himalayas, Pakistan*

The Himalayan main frontal thrust (MFT) accommodates most of the present-day Indo-Asia convergence. The seismicity and deformation mechanism varies considerably across the frontal Himalayas. We mapped a segment (Manzai Ranges) of the MFT at the western margin of the Himalayas and analyzed its deformation mechanism and active tectonics using geomorphic indices and the Interferometric Synthetic Aperture Radar (InSAR) Small Baseline Subset (SBAS) technique. Two frontal thrust faults were mapped using Sentinel-2B data. The C-band RADAR interferometry (Sentinel-1A) showed an average uplift of 5–9 mm/year in the satellite line of sight (LOS) from May 2018 to October 2019. The velocity profiles show an uplift variation across the anticlines and may be related to the displacement transfer from the zone of compression in the Manzai Ranges to the zone of transpression in the Pezu-Bhittani Ranges. To assess the relative tectonic activity, normalized longitudinal river profile and normalized channel steepness index (K<sub>sn</sub>) were calculated. The landscape response to active tectonics in the study area demonstrate a deep fluvial, convex river profiles, topographic breaks as knickpoints, and a high K<sub>sn</sub> index. The geomorphic parameters show a relative increase in tectonic uplift and deformation from the Kundi anticline to the Khirgi and Manzai anticline. This work suggests that the frontal structures in the western Himalayas are still going through an active phase of deformation and landscape development with both seismic and aseismic creep.

**Sean Romito***Testing the transitional crust and its implications on the tectonomagmatic evolution of the Camamu-Almada margin along the northeastern rift segment of Brazil*

The Camamu-Almada 100-km-wide margin covers an area of 22,000 km<sup>2</sup> and includes: 1) thin (25 km-thick) to ultra-thin (5 km-thick) metamorphic continental crust; 2) transitional crust of unknown composition (4–8 km-thick); and 3) Albian and younger oceanic crust (6–8 km-thick). Hypotheses for the composition of the transitional zone include: 1) normal oceanic crust, 2) unroofed lower continental crust, 3) exhumed mantle, and 4) volcanic or incipient oceanic crust. We investigate the structural-magmatic evolution of the Camamu and Almada by interpreting 19,000 line-km of 2D reflection seismic, including two long-offset PSDM transects recorded to a depth of 40 km, 105 offshore well logs, regional magnetic and gravity grids, and 15 seismic refraction stations. Seismic interpretation and 2D gravity models suggest that the transitional zone is structurally complex and composed of at least three crustal blocks: a 30 km-wide central block that is either high-density (>3.1 g/cc) or thin (<4 km-thick), flanked by two 50 km-wide, 4–8 km-thick, lower-density (2.7–2.9 g/cc) blocks. 3D gravity models reveal the areal extents of these zones and heavily implies that the central block is high-density, rather than thin. We propose a Camamu-Almada transitional zone succession of, from west to east: 1) 0–40 km-wide unroofed lower continental crust, 2) 20 km-wide exhumed mantle, and 3) 40–60 km-wide incipient oceanic crust.

### Stephanie Suarez

#### *Pb and Rb-Sr isotope systematics of enriched components in Tissint*

Acquiring isotopic data from Martian specimens, whether from meteorites or returned samples, is essential in understanding the evolution of Mars. Primary chemical and isotopic signals can be obscured through mobilization of elements during secondary Martian processes including impacts and fluid/rock interactions. Direct sample return or meteorite specimens from observed falls offer pristine examples of these Martian processes. Tissint, a shergottite that had minimal opportunity to undergo significant modification on Earth's surface, is used to explore primary characteristics related to igneous crystallization as well as element mobility related to ejection. Depleted shergottite Tissint is geochemically characterized as originating from an incompatible trace element (ITE)-depleted mantle source. Initial Sr, Nd, Hf, and Pb isotope compositions determined from isochron intercepts are some of the most depleted of any shergottite, however, solutions from weak acid washes of several whole rock specimens are relatively enriched in radiogenic Sr and Pb isotopic compositions compared to igneous minerals. It has been hypothesized that the sources of enrichment are Martian soils, but this is debated. Additional hypotheses include addition of Pb isotopes by fluids [6] and, or impact metamorphism. Multiple specimens of Tissint were analyzed in situ by LA-ICPMS for REE, highly siderophile element (HSE) concentrations, and Pb isotopic compositions. Leachate and residues from 8 specimens representing separate individual fragments were analyzed for Rb-Sr by TIMS. Analyses of Tissint did not reveal the presence of exogenous materials as previously hypothesized. REE and HSE concentrations and Pb isotopic compositions confirm that the enriched components are not hosted in mineral phases or impact glass and associated sulfide.  $87\text{Rb}/87\text{Sr}$  analyses of leachates indicate that labile components hosting soluble Rb and Sr are not in isotopic equilibrium with the igneous assemblage. The Sr isotopic compositions of the leachate are within the range of 'more enriched' depleted shergottites, perhaps indicating sources from the igneous pile on Mars. The enriched component could represent crack and mineral surface coatings of volatilized materials derived from nearby depleted shergottite rock units during the impact ejection process.

### Osman Tirmizi

#### *Hazard Potential in Southern Pakistan: A Study on the Subsidence and Neotectonics of Karachi and Surrounding Areas*

Coastal communities in deltaic regions around the world are subject to subsidence through a combination of natural and anthropogenic. The city of Karachi in southern Pakistan is situated along the diffuse western boundary of the tectonically active Indian Plate, making it more susceptible to natural subsidence processes from plate motion-related deformational events such as earthquakes and faulting. Excessive abstraction of groundwater, extensive groundwater use in irrigation, and construction of upstream dams and barrages are some of the anthropogenic contributions to subsidence in the area. A combination of the lack of historic data and few previous studies in the area make it difficult to determine the rate. We present an integrated study of the subsidence and neotectonic activity of Karachi and its surrounding areas using static GPS survey data and Interferometric Synthetic Aperture Radar (InSAR) time-series techniques to determine the severity and extent of deformation. Positional time-series analysis of the static GPS survey data reveals a displacement of approximately 32.5 cm in the north direction, 38 cm in the east direction, and 2 cm down in the vertical direction over the course of 10 years. These average to about 3.25 cm, 3.8 cm, and 0.2 cm displacements per year in the north, east, and vertical directions respectively. The InSAR results for satellite LOS velocity change in both ascending and descending tracks indicate movement away from the satellite in key residential and industrial areas. Further decomposition into 2 dimensions (east-west and vertical) quantifies displacement in these areas to about 1cm to  $\geq 3\text{cm}$  downward per year. Karachi is one of the most densely populated cities in the world, with an estimated population of over 16 million people. Determining the rate of subsidence and extent of neotectonic activity is crucial for mitigating seismic hazard.

### Weiyao Yan

#### *A new concordia age for the 'forearc' Bay of Islands Ophiolite Complex, Western Newfoundland utilizing spatially resolved LA-ICP-MS U-Pb analyses of zircon*

Advancements of zircon U-Pb dating techniques using laser ablation-inductively coupled plasma-mass spectrometry (LA-ICP-MS) provide an opportunity to precisely constrain the age of the Bay of Islands Ophiolite Complex (BOIC) in the Newfoundland Appalachians. New LA-ICP-MS U-Pb dates are presented for a large population of relatively simple magmatic zircon grains from trondhjemites using selective domain analyses and a 3% discordance filter in five samples collected from a single ophiolite massif, with four of the samples from a single pluton. All samples were derived from plagiogranite plutons intruded just below the gabbro-sheeted dike contact of the Blow Me Down Mountain massif, the massif sampled for three of the four prior single sample ID-TIMS age studies of the ophiolite. A highly consistent series of LA-ICP-MS concordant ages from the five samples collected yield a composite concordia age of  $488.3 \pm 1.5$  Ma, which we propose for the revised igneous age of the ophiolite massif. This new age for the BOIC is based on 127 individual LA-ICP-MS zircon analyses and is slightly older and with lower uncertainty than the previous consensus age. We review previous pioneering ID-TIMS U-Pb dates, ages, intercept assumptions, and uncertainties for the BOIC in light of this new formation age. Legacy ages and uncertainties differ somewhat when data are reduced with modern recommended techniques and without geological interpretations that fix lower intercepts. The ca. 488.3 Ma BOIC age indicates its formation along a younger supra-subduction forearc trench-orthogonal spreading center that rifted the older Coastal Complex forearc ophiolitic assemblages reported to be formed at ca. 500-508 Ma. This rifted forearc is analogous to many modern ophiolitic forearcs. The BOIC age is highly correlated with similar ages of the peri-Laurentian Notre Dame arc-proximal Betts Cove and Point Rouse ophiolites, indicating temporal BOIC spreading center linkages within the Baie Verte Oceanic Tract.



**Hualing Zhang***Integration of basin analysis and gravity modeling for the Sergipe-Alagoas rifted-passive margin, northeastern Brazil*

The coastal area and shelf of the Sergipe-Alagoas Cretaceous, rifted-passive margin, has been explored for hydrocarbons since 1935. Exploration has focused on deepwater (~2 km water depths) and ultra-deepwater (up to 2.5 km) plays since 2007 and made this area of the Brazilian margin a very promising frontier for ultra-deepwater exploration. The structural framework of the Aptian rifted margin consists of NE-striking normal fault systems with subsidiary E-W and NW-SE faults that are interpreted as transfer faults. We investigate the crustal architecture and the nature of the continental-oceanic boundary (COB) of the study area by integrating conventional 2D and deep-penetration ION Span lines with well log interpretations and regional 2D gravity modeling. Results include: 1) the continental crust thins from 15-25 km in the mountainous coastal area to 10-15 km within necked zone landward of the COB; 2) the upper oceanic crust forms a 3-km-thick zone of seismic transparency, which is inferred to consist of pillow basalts; 3) the 5-km-thick lower, continental crust is characterized by high-amplitude reflectors dipping landward and seaward, which are interpreted to be gabbroic dikes crosscutting a larger volume of sheeted dikes; 4) a marginal rift filled by both seaward-dipping reflectors (SDRs) and clastic sedimentary rocks separate the 8-km-thick, thinned continental crust from 8-km-thick oceanic crust; 5) Late Cretaceous and Cenozoic hotspot-related seamounts thicken the oceanic crust by 40% relative to the oceanic crust to the southern part of the study area that is less affected by hotspot activity; 6) volcanoes making up the NW-SE-trending Romano Russo and Klenova seamount chain in the southeastern area are mapped in detail using gravity filters as are the extent of volcanic SDRs concentrated in the northwestern Sergipe sub-basin; 7) oceanic fracture zones are shown as linear, EW gravity highs on the residual Bouguer gravity map and as lows on the magnetic map; and 8) basin modeling in the central Sergipe basin shows that the Albian source rock entered the oil window in the early Paleocene; areas with mature source rocks correlate well with a band of thinned continental crust overlain by 4 km of sedimentary overburden.



*Hualing Zhang*

**STUDENT RESEARCH CONFERENCE CHAIR**

I am a third-year Ph.D student working with Dr. Paul Mann. I completed my master's degree, which focused on deep-water petroleum system exploration in the Midland Basin, at the University of Texas at Austin. My research involves the integration of regional gravity modeling, sequence stratigraphy, and basin analysis for understanding the tectonic and hydrocarbon evolution of the Permian Basin (west Texas) and the Sergipe-Alagoas rifted-passive margin (Brazil).



*Lucien Nana Yobo*

**GRADUATE STUDENT CHAIR & GEOLOGY REPRESENTATIVE**

I obtained a B.S. in geology from Fresno State and an M.S. in geology from the University of Nebraska. I am currently a final-year PhD candidate at the University of Houston. My research involves using multi-isotope proxy to understand the cause and expansion of anoxia during ocean anoxic event 2. When not studying, I love to read and engage in dialogue about governance and leadership in Africa.



*Madeline Statkewicz*

**ATMOSPHERIC SCIENCE REPRESENTATIVE & CONTENT CREATOR**

I am a third-year Ph.D. candidate in atmospheric science working under the advisory of Dr. Bernhard Rappenglueck and previously worked with the late Dr. Robert Talbot. Previously, I earned my B.S. in applied mathematics and minor in physics from the University of South Alabama. My work concerns the impact of changing precipitation patterns on flooding in Houston, a rapidly growing urban area. I am also interested in science policy and communication.



*Rachel Clark*

**EVENT COORDINATOR**

I am a fourth-year Ph.D. candidate working under the guidance of Dr. Julia Wellner. Before coming to UH, I received a bachelor's degree in geology from Bryn Mawr College. My research experiences have covered various topics in marine geology and geophysics for both tropical and polar regions. For my doctoral research, I sail to the Amundsen Sea in West Antarctica to collect marine sediment cores. I use these sediment cores to reconstruct glacial history in this rapidly changing region of Antarctica. Starting this year, I have taken an interest in sharing what I've learned so far about polar science with local community groups and schools.



*Sharif Morshed*

**GEOPHYSICS REPRESENTATIVE**

I am a final-semester doctoral student working with Dr. Evgeny Chesnokov. I received a master's in Geoscience from the University of Texas at Austin and a bachelor's degree in geology from the University of Dhaka (Bangladesh). Previously I worked for Task Fronterra Geosciences as a geologist and for Lumina Geophysical as a reservoir geophysicist. My work and research expertise includes petrophysics, rock physics, and reservoir geomechanics. My PhD topic is "stress and frequency-dependent properties of anisotropic poroelastic rocks."



*Joseph McNease*

**UNDERGRADUATE REPRESENTATIVE**

I am a third-year undergraduate geophysics major with a minor in mathematics. I am currently doing research with Aramco's geophysics research and development team on near surface noise attenuation using conditional generative adversarial networks. I am interested in solid earth geophysics, machine learning for seismic data analysis and interpretation, and science education. When I am not studying or working, I like to play chess, program, and solve math problems.

We would like to thank all who volunteered as judges for this event, whether from EAS faculty and staff, industry guests, University of Houston Alumni, or some combination therein. The Student Research Conference would not be what it is without you!

<b>1</b>	Arpana Sarkar	<i>Industry Guest</i>
<b>2</b>	Bernhard Rappenglueck	<i>EAS Faculty</i>
<b>3</b>	Caroline Wilkinson	<i>Industry Guest</i>
<b>4</b>	Courtney Anzalone	<i>Industry Guest @ UH Alumni</i>
<b>5</b>	Di Chen	<i>UH Alumni</i>
<b>6</b>	Emily Beverly	<i>EAS Faculty</i>
<b>7</b>	Fatemeh Afshar Ghahremani	<i>Guest</i>
<b>8</b>	Gary Guthrie	<i>Industry Guest</i>
<b>9</b>	Gavin Menzel-Jones	<i>Industry Guest</i>
<b>10</b>	George Zhao	<i>Industry Guest</i>
<b>11</b>	Jinny Sisson	<i>EAS Faculty</i>
<b>12</b>	Kirstie Haynie	<i>UH Alumni</i>
<b>13</b>	Martin Cassidy	<i>EAS Faculty @ UH Alumni</i>
<b>14</b>	Mehmet Tanis	<i>Industry Guest</i>
<b>15</b>	Minako Righter	<i>EAS Faculty</i>
<b>16</b>	Ny Riavo Voarintsoa	<i>EAS Faculty</i>
<b>17</b>	Parekh Chirag	<i>UH Alumni</i>
<b>18</b>	Robert Stewart	<i>EAS Faculty</i>
<b>19</b>	Rosemarie Geetan	<i>UH Alumni</i>
<b>20</b>	Shawn Wright	<i>Industry Guest @ UH Alumni</i>
<b>21</b>	Weiguo Li	<i>UH Alumni</i>
<b>22</b>	Xun Jiang	<i>EAS Faculty</i>
<b>23</b>	Yi-An Lin	<i>EAS Staff @ UH Alumni</i>
<b>24</b>	Yiduo Liu	<i>EAS Staff @ UH Alumni</i>
<b>25</b>	Yunsoo Choi	<i>EAS Faculty</i>



We would also like to thank and acknowledge the College of Natural Science and Mathematics for their contributions to the 2021 Student Research Conference. Thank you for your support!

U N I V E R S I T Y of  
**HOUSTON**

---

COLLEGE of NATURAL SCIENCES & MATHEMATICS

# WHO ARE WE?


The Department of Earth and Atmospheric Sciences at the University of Houston has a wide range of research programs central to the earth sciences.

Air Pollution	Isotope Geochemistry
Air Quality	Marine Geology
Applied Geophysics	Micropaleontology
Applied Rock Physics	Potential Fields
Atmospheric Science	Remote Sensing
Carbonate Petrology	Sedimentology
Climatology	Seismology
Geodynamics	Sequence Stratigraphy
GIS	Structural Geology
Hydrology	Tectonics
Igneous Petrology	Thermochronology
Inorganic Geochemistry	Whole Earth Geophysics

The Department offers M.S. and Ph.D. degrees in Geology, Geophysics, and Atmospheric Sciences, a B.S. in Geology, Geophysics, and Environmental Sciences, and a B.A. in Earth Sciences. Fieldwork is a major component of all degree programs. The Department also offers Professional M.S. programs in Petroleum Geology and Petroleum Geophysics that are offered at convenient hours for professional geoscientists working in industry or aspiring for a professional position within the petroleum industry.

## CONTACT US

Department of Earth and Atmospheric Sciences  
4800 Cullen Boulevard, Houston, TX 77204

 (713) 743-3399

 <http://www.eas.uh.edu>